Neurocomputing 157 (2015) 187–198

Contents lists available at ScienceDirect

Neurocomputing

journal homepage: www.elsevier.com/locate/neucom

Probability iterative closest point algorithm for *m*-D point set registration with noise

Shaoyi Du [a,*], Juan Liu [a], Chunjia Zhang [a], Jihua Zhu [a], Ke Li [b]

[a] Institute of Artificial Intelligence and Robotics, Xi'an Jiaotong University, Xi'an 710049, China
[b] The Fundamental Science on Ergonomics and Environment Control Laboratory, Beihang University, Beijing 100191, China

ARTICLE INFO

Article history:
Received 28 October 2014
Received in revised form
25 December 2014
Accepted 11 January 2015
Communicated by Rongrong Ji
Available online 19 January 2015

Keywords:
Iterative closest point
Point set registration
Noise
Gaussian model
One-to-one correspondence

ABSTRACT

This paper proposes probability iterative closest point (ICP) method based on expectation maximization (EM) estimation for registration of point sets with noise. The traditional ICP algorithm can deal with rigid registration between two point sets effectively, but it may fail to register point sets with noise. In order to improve the registration precision, a Gaussian model is introduced into the traditional rigid registration problem. At each iterative step, similar to the original ICP algorithm, there are two parts of the proposed method. Firstly, the one-to-one correspondence between two point sets is set up. Secondly, the rigid transformation is solved by singular value decomposition (SVD) method, and then the Gaussian model is updated by the distance and variance between two point sets. The proposed method improves the precision of registration of point sets with noise significantly with fast speed. Experimental results validate that the proposed algorithm is more accurate and faster compared with other rigid registration methods.

1. Introduction

In pattern recognition and computer vision, various features are applied widely [1,2], especially the point set representing position is a common feature. Therefore, point set registration has become a very important and basic research topic for its wide application. The goal of registration is to find the corresponding relationship between two point sets and compute an appropriate transformation with which the shape point set can register to the model point set. The typical method is the iterative closest point (ICP) algorithm which offers a good solution to the point set registration [3–5]. The ICP algorithm has been widely used in many fields for its advantages of high speed and precision. Moreover, some scholars have also extended the rigid registration to the non-rigid case, including scale [6], affine [7] and nonlinear registration [8].

In the past few decades, many researchers have devoted great efforts to rigid registration of traditional point sets, especially on the speed and robustness. To speed up the ICP algorithm, Xu et al. [9] introduced five constraint conditions of registration point pairs, and Kim et al. [10] proposed two acceleration techniques: hierarchical model point selection and logarithmic data point search. A combination of ICP variants was able to align two range images in a few tens of milliseconds, but it needed a good initial guess for high speed [11]. The Levenberg–Marquardt algorithm which was general-purpose non-linear optimization was adopted to accelerate the ICP [12]. Jost et al. [13] proposed a solution combining a coarse to fine multiresolution approach with the neighbor to speed up the ICP. Meanwhile, there were also many researchers studying the robustness of ICP. Almhdie et al. [14] presented an enhanced implementation of the popular ICP algorithm for the registration of 3D free-form closed surfaces, which was based on the use of a look up matrix for finding the best correspondence pairs. Zhang et al. [15] presented a more robust ICP approach for 2D point set registration and an inequality constraint of the rotation angle was introduced into the registration model which was solved by an extended ICP algorithm. Invariant features decreased the probability of being trapped in a local minimum [16]. Lee et al. proposed a matrix which represented the reliability of the rotation components of ICP [17]. Biunique correspondence [18] was introduced to enhance the performance of ICP by searching multiple closest points and the algorithm could find the correct rigid transformation with the existence of large non-overlapping area and poor initial alignment. Silva et al. [19] introduced a new hybrid genetic algorithm technique and evaluation metric based on surface interpenetration to improve the robustness.

It should be pointed out that the above mentioned approaches could not handle the point sets with a large number of outliers and

* Corresponding author. Tel.: +86 29 82668672.
E-mail address: dushaoyi@gmail.com (S. Du).

http://dx.doi.org/10.1016/j.neucom.2015.01.019
0925-2312/

noise which exist widely in application. To solve the registration of point sets with outliers, many researchers made great efforts. Some matched corresponding points based on overlapping percentage. The trimmed ICP algorithm which incorporated an overlapping percentage into a least square function to trim outliers was proposed [20]. Nevertheless, the algorithm was time-consuming. Hence, the fractional ICP which simultaneously computed the best transformation and the overlapping percentage could identify and discard outliers, and achieved fast speed [21]. However, this method depended greatly on the parameter. Thus, Du et al. [22] proposed a novel objective function which could automatically compute rigid transformation, correspondence, and overlapping percentage without influence of a parameter. Meanwhile, the distance threshold was also discussed. Rodriguez-Losada [23] presented a technique to improve the data association in the ICP based on a distance-filter adopting the idea of a coarse estimation of the correct solution, which could be used to test each single association and robustly discard wrong ones. A modified ICP method was proposed to ameliorate the performance of laser scan alignment by applying dynamic distance error threshold [24]. Ridene and Goulette proposed a variant of ICP based on an adaptive dynamic threshold and a RANSAC method was used to remove outliers [25].

The above-mentioned approaches are effective for outliers, but they are not suitable for dealing with point sets with noise which is always produced due to the precision of the acquisition equipment in the real application. The acquired data may have different precisions and random noise, so some researchers proposed to join probability into the ICP algorithm to improve the rigid registration precision [26–28], and the coherent point drift algorithm [28] extends to the non-rigid registration. Each of the point sets was represented by a mixture of Gaussians and the point set registration was treated as a problem of aligning the two mixtures [26]. A new method corresponded to ICP with multiple matches weighted by normalized Gaussian weights, gives birth to the EM–ICP using expectation maximization (EM) principle [27], which adopts full correspondence relationship for all the points in the model point set and the shape point set. Hence, it is time-consuming and the precision is limited due to the true correspondence being disturbed by the unimportant points which are the false corresponding points. To cope with this problem, we use the EM principle and adopt one-to-one correspondence which is for all the points in the shape point set only needed to find the closest points from the model set. The one-to-one correspondence is able to suppress the unimportant points and retain the original information of point pairs without the interference of noise, and therefore this method achieves high accuracy. However, the one-to-one correspondence may cause the proposed algorithm trapped into the local minimum, so the variance of Gaussian probability model is updated from large to small step by step, which makes the registration from coarse to fine. In the beginning the variance is given a big value, so all the points are approximate to uniform distribution which is the coarse registration. As the variance becomes small, the distribution gets close to the true distribution of the registration error which is the fine registration. As the proposed method adopts the one-to-one correspondence and the variance is updated from large to small, it achieves the fast speed and high accuracy.

This paper is organized as follows. Section 2 briefly reviews the process of the original ICP. Following that is Section 3, aiming at solving the rigid registration of point sets with noise, the Gaussian probability model is introduced and the probability iterative closest point algorithm is proposed. In Section 4, the validity and convergence property are analyzed. Experimental results on part B of CE-Shape-1 and the Stanford 3D Scanning Repository databases are present in Section 5. Finally, the conclusion is given in Section 6.

2. Iterative closest point algorithm

For the rigid registration of point sets, ICP is the typical algorithm proposed by Besl and McKay [3–5], which has been widely used in various research fields for its fast speed and high precision.

Given two point sets in $\mathbb{R}^n$: the shape point set $X=\{\vec{x}_i\}_{i=1}^{N_x}(N_x\in\mathbb{N})$ and the model point set $Y=\{\vec{y}_j\}_{j=1}^{N_y}(N_y\in\mathbb{N})$, in order to guarantee the consistency of the shape point set and the model point set in Euclidean distance space, the ICP algorithm is employed to solve the rigid transformation. For the registration of these two point sets, least square (LS) is used to measure and the formula can be expressed as follows:

$$\min_{\mathbf{R},t,j\in\{1,2,\cdots,N_y\}}\left(\sum_{i=1}^{N_x}\|(\mathbf{R}\vec{x}_i+t)-\vec{y}_j\|_2^2\right)$$
$$\text{s.t.}\quad \mathbf{R}^T\mathbf{R}=I_n,\det(\mathbf{R})=1 \tag{1}$$

The procedure of the ICP algorithm includes two steps. At each iterative step, correspondence is set up by finding the model points which are the closest to the shape point set, and then the rigid transformation is obtained. The main steps of ICP are summarized as follows:

(1) According to the obtained rigid transformation of $(k-1)$th step, the shape point set will be transformed by rotation matrix $\mathbf{R}_{k-1}$ and translation vector t_{k-1}. After transformation, correspondence between two point sets is established as follows:

$$c_k(i)=\arg\min_{j\in\{1,2,\cdots,N_y\}}(||(\mathbf{R}_{k-1}\vec{x}_i+t_{k-1})-\vec{y}_j||_2^2),i=1,2,\cdots,N_x \tag{2}$$

(2) For the shape point set $\{\vec{x}_i\}_{i=1}^{N_x}$ and the corresponding model point set$\{\vec{y}_{c_k(i)}\}_{i=1}^{N_x}$, we need to solve new rigid transformation between them as follows:

$$(\mathbf{R}_k,t_k)=\arg\min_{\tilde{\mathbf{R}}_k{}^T\tilde{\mathbf{R}}_k=I_n,\det(\tilde{\mathbf{R}})=1,\tilde{t}_k}\left(\sum_{i=1}^{N_x}||\tilde{\mathbf{R}}_k\vec{x}_i+\tilde{t}_k-\vec{y}_{c_k(i)}||_2^2\right) \tag{3}$$

Steps (1) and (2) are repeated until the iteration is convergent. As the method is a local convergent method, initial values of rotation matrix and translation vector are important. Good initial values not only guarantee the algorithm converges to the global minimum value, but also greatly improve the efficiency of computation. The selection of initial values also has a lot of methods [3,29,30], which is not detailedly analyzed here.

3. Probability iterative closest point algorithm

3.1. Problem statement

ICP 相对来说肯定是非常精确的，但是实际的模型是夹杂噪声的。

The traditional ICP algorithm can accomplish the rigid registration with good accuracy and fast speed, but it fails to register two point sets with noise named noisy point sets. The noise got by the sensor or produced by the image processing is called shape noise. Fig. 1 presents a registration result of 2D noisy point sets.

In Fig. 1, the red points show one shape without noise, while the blue points show the noisy point set. Through the ICP registration result, it is obvious to see that the noisy points on the edge will influence the result of registration significantly. Due to the interference of noise, the shape boundaries after registration will not be completely aligned, so Gaussian probability model is

为什么总是高斯模型?

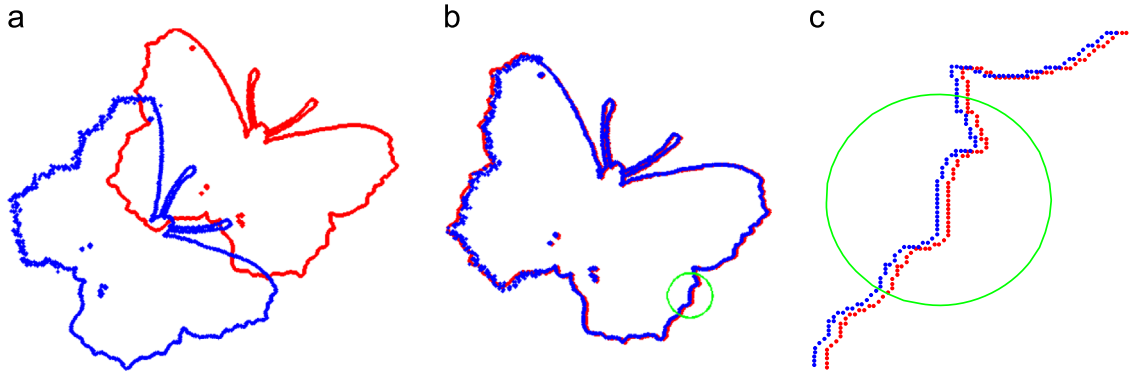

Fig. 1. Point sets of different shapes. (red: point set is without noise, blue: point set is the noisy point set) (a) 2D Butterfly. (b) Registration result of ICP. (c) Amplification result of the green area. (For interpretation of the references to color in this figure legend, the reader is referred to the web version of this article.)

introduced. The probabilities between shape point set and model point set are real-time calculated in each iteration. On the whole the distances of noisy points are far, so probabilities calculated by Gaussian model are small. In this way, noisy points contribute little to the registration result which meets our expectation.

The registration between two point sets with noise is considered as a probability density estimation problem. According to law of total probability, the probability formula of shape point set is as follows:

$$p(\vec{x}) = \sum_{j=1}^{N_y} P(\vec{y}_j) p(\vec{x} \mid \vec{y}_j). \tag{4}$$

For shape point set and model point set satisfying the Gaussian probability model, the following formula is used to show their relationship:

$$p(\vec{x} \mid \vec{y}) = \frac{1}{(2\pi\sigma^2)^{n/2}} \exp^{-\frac{||T(\vec{x})-\vec{y}||_2^2}{2\sigma^2}} \tag{5}$$

where n is the dimension of point sets, σ^2 is the variance of the Gaussian probability model and $||T(\vec{x})-\vec{y}||_2^2$ shows the distance between the transformed shape point set $T(\vec{x})$ and the model point set $\vec{y}$.

According to (5), it can be seen that probability formula is Gaussian distribution with zero mean and σ^2 variance. Because $-||T(\vec{x})-\vec{y}||_2^2$ is the exponent of the exponential function which is negative, the shorter the distance of the transformed shape point set and the model point set is, the greater the Gaussian probability is and vice versa. The distances of noisy points are far as a whole, so the weights are small, thus it can gradually reduce the influence of noise, and achieves satisfactory registration result.

To simplify the model, we assume that the model point set subjects to the uniform distribution, so

$$P(\vec{y}) = \frac{1}{N_y}. \tag{6}$$

Because Gaussian probability model is introduced, the variance σ^2 can be seemed as a parameter which is considered for its influence on accuracy and speed for maximum-likelihood (ML) estimation. The objective function of the likelihood function is given as follows:

$$\begin{aligned} F(\vec{x}; \mathbf{R}, t, \sigma^2) &= -\sum_{i=1}^{N_x} \log\ p(\vec{x}_i \mid \mathbf{R}, t, \sigma^2) \\ &= -\sum_{i=1}^{N_x} \log \sum_{j=1}^{Ny} P(\vec{y}_j) p(\vec{x}_i \mid \vec{y}_j, \mathbf{R}, t, \sigma^2). \end{aligned} \tag{7}$$

3.2. Probability ICP algorithm

In this paper, we study the rigid registration for noisy points. Similar to the EM–ICP algorithm [27], we also introduce the EM principle to the ICP algorithm to solve the problem (7). EM consists of two steps: E-Step and M-Step. Hence the proposed algorithm is also composed of two parts. During the E-Step, the one-to-one correspondence is established between the shape point set and the model point set. M-Step is to solve the new rigid transformation based on E-Step and the probability of corresponding points using the SVD method, and then the posterior Gaussian probability is calculated according to the distance and variance between two point sets. Establishing the one-to-one correspondence between two point sets can greatly reduce the computing time and achieve high accuracy as it is able to suppress the unimportant points and retain the original information of point pairs without the interference of noise. Moreover, the variance of Gaussian probability model is updated from large to small step by step, which can make the registration from coarse to fine to prevent the proposed algorithm from being trapped into the local minimum.

EM algorithm is used to solve (7) including E-Step and M-Step:

E-Step: Based on the rigid transformation of $(k-1)$th step, the correspondence of kth step is established adopting one-to-one correspondence which is for each shape point to find the nearest model point:

$$c_k(i) = \arg\min_{j \in \{1,2,\ldots,N_y\}} \sum_{i=1}^{N_x} ||\mathbf{R}_{k-1}\vec{x}_i + t_{k-1} - \vec{y}_j||_2^2 \tag{8}$$

For the objective function (8), Delaunay triangulation [31,32], k–d tree [33,34] and linear deviation searching [35,36] are common closest point search strategies, and in this paper the first method is employed.

M-Step: The posterior probability got by (15) is employed as the probability, and the initial variance is given a big value, so it can be assumed that the initial distribution is uniform distribution. As correspondence and corresponding Gaussian probability are known, (7) is used to establish a new objective function. By maximizing the objective function, the new rigid transformation $(\mathbf{R}_k, t_k)$ and variance σ_k^2 is solved. The new objective function is established as follows:

$$\begin{aligned} M(\tilde{\mathbf{R}}_k, \tilde{t}_k, \tilde{\sigma}_k^2) = &\sum_{i=1}^{N_x}\sum_{j=1}^{N_y} p(\vec{y}_j \mid \vec{x}_i, \mathbf{R}_{k-1}, t_{k-1}, \sigma_{k-1}^2) \\ &\times \log\left(P(\vec{y}_j) p(\vec{x}_i \mid \vec{y}_j, \tilde{\mathbf{R}}_k, \tilde{t}_k, \tilde{\sigma}_k^2)\right). \end{aligned} \tag{9}$$

As the one-to-one correspondence is adopted, the probability is not zero only when $j=c_k(i)$, so (9) can be simplified as follows:

$$M(\tilde{\mathbf{R}}_k,\tilde{t}_k,\tilde{\sigma}_k^2)=\sum_{i=1}^{N_x} p(\vec{y}_{c_k(i)}|\vec{x}_i,\mathbf{R}_{k-1},t_{k-1},\sigma_{k-1}^2)\times\log(P(\vec{y}_{c_k(i)})p(\vec{x}_i|\vec{y}_{c_k(i)},\tilde{\mathbf{R}}_k,\tilde{t}_k,\tilde{\sigma}_k^2)). \tag{10}$$

Let $p_i^{k-1}=p(\vec{y}_{c_k(i)}|\vec{x}_i,\mathbf{R}_{k-1},t_{k-1},\sigma_{k-1}^2)$, and the new target function is got by simplifying (10) using (5) and (6) with an additional probability (15)

$$M(\tilde{\mathbf{R}}_k,\tilde{t}_k,\tilde{\sigma}_k^2)=-\sum_{i=1}^{N_x} p_i^{k-1}\times\frac{||\tilde{\mathbf{R}}_k\vec{x}_i+\tilde{t}_k-\vec{y}_{c_k(i)}||_2^2}{2\tilde{\sigma}_k^2}-\sum_{i=1}^{N_x} p_i^{k-1}\times\log(N_y(2\pi\tilde{\sigma}_k^2)^{\frac{n}{2}}). \tag{11}$$

Because of only the first part related to the rotation matrix and translation vector, maximizing above formula is equivalent to maximizing $-\sum_{i=1}^{N_x} p_i^{k-1}\times||\tilde{\mathbf{R}}_k\vec{x}_i+\tilde{t}_k-\vec{y}_{c_k(i)}||_2^2/2\tilde{\sigma}_k^2$ with respect to the rotation matrix and translation vector, so the goal is to solve the following function:

$$(\mathbf{R}_k,t_k)=\underset{\tilde{\mathbf{R}}_k^T\tilde{\mathbf{R}}_k=I_n,\det(\tilde{\mathbf{R}}_k)=1,\tilde{t}_k}{\arg\min}\sum_{i=1}^{N_x} p_i^{k-1}\times||\tilde{\mathbf{R}}_k\vec{x}_i+\tilde{t}_k-\vec{y}_{c_k(i)}||_2^2 \tag{12}$$

The formulation of (12) is similar to that of the classical ICP algorithm just more than a probability p_i^{k-1}, which can be solved by the SVD method. As the probability is introduced in this paper, we define the root mean square (RMS) error as $(\sum_{i=1}^{N_x} p_i\times||\mathbf{R}_k\vec{x}_i+t_k-\vec{y}_{c_k(i)}||_2^2)^{0.5}$. The estimated variance of EM adopts solving the derivation of $M(\mathbf{R}_k,t_k,\tilde{\sigma}_k^2)$ based on the variance and the derivation is 0 corresponding to the variance desired. The estimated variance of EM is obtained as follows:

$$\hat{\sigma}_k^2=\sum_{i=1}^{N_x} p_i^{k-1}\times\frac{||\mathbf{R}_k\vec{x}_i+t_k-\vec{y}_{c_k(i)}||_2^2}{n}. \tag{13}$$

The estimated variance of EM $\hat{\sigma}_k^2$ obtained from (13) is actually the registration error of kth step. After getting the estimated variance of EM, (14) is used to update the variance of the Gaussian probability

$$\sigma_k^2=\begin{cases}\sigma_{k-1}^2/\lambda & \sigma_{k-1}^2/\lambda>\hat{\sigma}_k^2\\ \hat{\sigma}_k^2 & \sigma_{k-1}^2/\lambda<\hat{\sigma}_k^2\end{cases} \tag{14}$$

λ is called annealing coefficient. When λ is 1, it is a special case which is not updating the variance, so it is standard ICP algorithm. When λ is big, it can improve the convergence speed, but it is also easy to fall into local minimum. Therefore, the value of λ ranges from 1 to 2 which is selected by experiments. To make full use of information of all points preventing the algorithm from being trapped in local minimum, the updating of variance adopts the idea of from coarse to fine. In the beginning the variance is given a big value, so all the points are approximate to uniform distribution, and σ_{k-1}^2/λ is used to change the variance of the Gaussian probability model from large to small step by step. When the two point sets are roughly registered, the probability-ICP (PICP) distinguishes between noisy points and effective points according to the distance and variance between two point sets. Hence the estimated variance of EM which is actually the registration error of last step is employed to precisely update the variance of the Gaussian probability model. The distances of noisy points are far as a whole, so the weights are small. Thus it can gradually reduce the influence of noise, and achieves satisfactory registration result.

Using $\mathbf{R}_k$, t_k and σ_k^2 of this step, the posterior Gaussian probabilities are updated between corresponding points and the weights are calculated

$$p(\vec{y}_{c_k(i)}|\vec{x}_i,\mathbf{R}_k,t_k,\sigma_k^2)=\frac{1/(2\pi\sigma_k^2)^{\frac{n}{2}}\exp^{-||(\mathbf{R}_k\vec{x}_i+t_k)-\vec{y}_{c_k(i)}||_2^2/\ 2\sigma_k^2}}{P} \tag{15}$$

where $P=\sum_{i=1}^{N_x} 1/(2\pi\sigma_k^2)^{\frac{n}{2}}\exp^{-||(\mathbf{R}_k\vec{x}_i+t_k)-\vec{y}_{c_k(i)}||_2^2/\ 2\sigma_k^2}$ is used to normalize the probability.

Establishing correspondence between all the points reduces the efficiency, so the one-to-one correspondence is used to find the model point nearest to the shape point. The one-to-one correspondence is able to suppress the unimportant points and retain the original information of point pairs without the interference of noise and can achieve high accuracy. To avoid the algorithm being trapped into local minimum, the variance of the Gaussian probability changes adopting the idea of from coarse to fine. The core of this algorithm is setting up the Gaussian probability model and updating it automatically, so the algorithm is named PICP, which is summarized in Table 1.

In the PICP algorithm, we use the one-to-one point correspondence instead of full correspondence of all point sets. To prevent the proposed algorithm from being trapped into the local minimum, the variance of Gaussian probability model is updated from large to small step by step, which can make the registration from coarse to fine. If the PICP algorithm adopts the estimated variance of EM to update the variance of Gaussian probability model from the start, the registration

Table 1
The general process of the proposed PICP algorithm.

Algorithm 1 The Proposed PICP Algorithm

1 Give the initial transformation $\mathbf{R}_0=\begin{bmatrix}1&0\\0&1\end{bmatrix}$ and $t_0=(0,0)^T$, set the value of $\lambda\in(1,2]$, and set the initial probability $p_i^0=\frac{1}{N_x}, i=1,2,...,N_x$.
2 Set $X=\mathbf{R}_0X+t_0$and the iterative index $k=0$.
3 **repeat**
4 $k=k+1$.
5 Set up the correspondence $c_k(i)$, $i\in\{1,2,\cdots,N_x\}$ via (8).
6 Solve the rotation matrix $\mathbf{R}_k$and translation vector $t_k$by SVD via (12).
7 Compute the variance between two point set by EM method via (13):
8 $\hat{\sigma}_k^2=\sum_{i=1}^{N_x} p_i^{k-1}\times\frac{||\mathbf{R}_k\vec{x}_i+t_k-\vec{y}_{c_k(i)}||_2^2}{n}$.
9 Update the variance of the Gaussian probability via (14):
$\sigma_k^2=\max(\sigma_{k-1}^2/\lambda,\hat{\sigma}_k^2)$.
10 Compute the posterior Gaussian probability by the rotation matrix $\mathbf{R}_k$, translation vector t_k and variance σ_k^2 via (15):$p_i^k=\frac{1/(2\pi\sigma_k^2)^{\frac{n}{2}}\exp^{-||(\mathbf{R}_k\vec{x}_i+t_k)-\vec{y}_{c_k(i)}||_2^2/\ 2\sigma_k^2}}{P}$
11 **until** $|RMS_k-RMS_{k-1}|<\varepsilon$or $k>Step_{\max}$.

process is very difficult to make full use of information of all points, and is easy to fall into the local minimum. Hence we first reduce variance through the constant proportion which is just the annealing coefficient λ until the two point sets are roughly matched. Then the estimated variance of EM further accurately updates the variance of Gaussian probability model which not only ensures high precision, but also has very good robustness.

At the end of each iteration, the algorithm needs to judge if it meets exiting conditions. If the difference between the RMS_k and RMS_{k-1} is smaller than a small number ε or the number of iteration reaches the given maximum value, the algorithm has reached the optimal minimum.

4. Theory analysis

In this section the convergence property and effectiveness of the proposed algorithm will be analyzed. As the EM algorithm is converged, this paper applies EM algorithm to finish point set registration effectively. In the E-step, it is equivalent to minimize the distance of each point pair under fixed probability, so the registration error decreases. In the M-step, the new transformation is solved by minimizing (12), which can also reduce the registration error. As the error decreases, it can be known that the variance σ_k^2 becomes smaller. Therefore, based on the property of Gaussian function, the probability of noisy points becomes smaller whose distances are far, and the probability of effective points becomes larger whose distances are short on the whole. As the sum of the probability is 1, the total registration error will reduce. Hence, the proposed algorithm usually converges to a local minimum after several iterative steps.

4.1. Establish one-to-one correspondence

In each iteration, EM–ICP algorithm builds full correspondence and calculates distance between all the points of shape point set and model point set, and then assigns the corresponding probability. Those processes can avoid the algorithm falling into local minimum, but it greatly increases the computation time and the accuracy is very limited. The reason is that the true correspondence is disturbed by the unimportant points which may be the false corresponding points. Hence, in PICP full correspondence is changed to be the one-to-one correspondence, where each point of the shape point set only needs to find the nearest point in the model point set and then a probability value is given. The one-to-one correspondence can exactly express the relationship of true point pairs with a large probability, while the probabilities of true point pairs given by full correspondence of the EM–ICP algorithm are relatively small for all other false points occupy some probabilities which decrease the accuracy. Thus, the one-to-one correspondence is able to suppress the unimportant points and retain the original information of point pairs without the interference of noise and can achieve high accuracy, but in order to prevent PICP algorithm from falling into local minimum, the Gaussian probability model is changed from large to small step by step, which can make the registration from coarse to fine.

The PICP algorithm can effectively avoid noise affecting the registration result, lying in the Gaussian probability model of (5). For effective points, distances are short, so they get large weight. For noisy points, distances are far, so they obtain small weight. On the overall, the noisy point is far away from the model point set, thus the weight is relatively small during matching. Therefore, the effective points have large weight and greatly contribute to the registration result, and comparatively the noisy points have small weight and contribute little to the registration result. In this way, the registration result can be completed satisfactorily.

4.2. Computing the rigid transformation by updating Gaussian probability model

In each iteration, when correspondence has been established, each corresponding pair gets posterior probability according to the distance between them. Assuming that expectation of the Gaussian probability model is 0, the variance is updated as a parameter. If the value calculated by (13) is adopted to update the variance of the Gaussian probability model at the beginning, it is easy to fall into local minimum value and the registration result is unsatisfied. Therefore, the variance of Gaussian probability model is varied from large to small step by step, which can make the registration from coarse to fine. To make full use of information, at the beginning uniform distribution is employed, that is, the weight and the contribution to each matching pair are the same. The variance of Gaussian probability model is updated by dividing by annealing coefficient until the value obtained by the EM method is bigger than the current variance. In this paper, the annealing coefficient of the PICP algorithm is chosen fixed in the interval (1, 2) manually. In fact, if it is larger than 2, the algorithm converges much faster, but it easily falls into a local minimum.

Based on the probability of the correspondence, we can compute the rigid transformation. It is clearly seen that the PICP algorithm is just more than a probability compared with the classical ICP algorithm, so the rigid transformation of PICP algorithm can also be solved by SVD, which can improve the precision of the registration results.

5. Experimental results

In this section, the PICP algorithm is compared with the ICP [3] and EM–ICP algorithms [27]. To demonstrate the precision of the PICP algorithm, we conduct the experiments on simulation and standard data including the part B of CE-Shape-1 [37] and the Stanford 3D Scanning Repository [38]. The errors of the compared

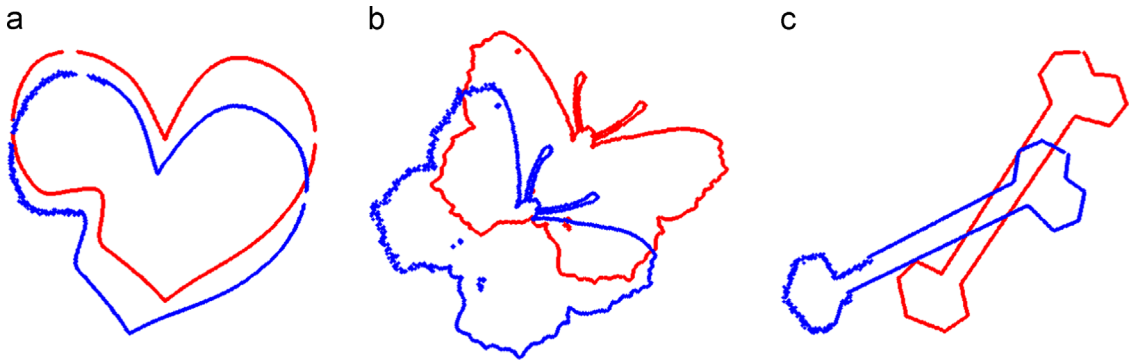

Fig. 2. The simulation data point set. (a) 2D Heart. (b) 2D Butterfly. (c) 2D Bone.

Table 2
Comparison of 2D simulation results.

Point sets	Angle		10	20	30	40	50	60
Heart	ICP	$\varepsilon_{\mathbf{R}}$	0.0061	0.0036	0.0016	3.7513e−4	0.0022	0.0040
		ε_t	0.1607	0.1279	0.0943	0.0963	0.1186	0.1439
		RMS	2.3204	2.2921	2.3153	2.3188	2.3157	2.2744
		Time(s)	0.1289	0.1294	0.1282	0.1227	0.1241	0.1284
	EM–ICP	$\varepsilon_{\mathbf{R}}$	0.0039	0.0028	3.2258e-4	0.0019	0.0030	0.0046
		ε_t	0.1019	0.0952	0.0586	0.0762	0.0932	0.1115
		RMS	1.3891	1.6475	1.4416	1.4865	1.5528	1.4270
		Time(s)	3.8632	3.8421	3.7826	3.7371	3.5945	3.3852
	PICP	$\varepsilon_{\mathbf{R}}$	1.2390e−5	1.0389e−5	1.4253e−5	9.8224e−6	1.2519e−5	5.1156e−6
		ε_t	3.3926e−4	2.9265e−4	3.9087e−4	2.7871e−4	3.2239e−4	1.3399e−4
		RMS	0.0565	0.0570	0.0608	0.0688	0.0681	0.0718
		Time(s)	0.1361	0.1347	0.1359	0.1259	0.1279	0.1340
Butterfly	ICP	$\varepsilon_{\mathbf{R}}$	0.0059	0.0043	0.0036	5.9563e−4	0.0018	0.0034
		ε_t	0.2740	0.1187	0.1306	0.1144	0.2118	0.1656
		RMS	2.2866	2.3368	2.3760	2.3434	2.3408	2.3808
		Time(s)	0.1272	0.1269	0.1255	0.1195	0.1192	0.1223
	EM–ICP	$\varepsilon_{\mathbf{R}}$	0.0045	0.0029	0.0019	1.0198e−5	0.0012	0.0025
		ε_t	0.1921	0.0788	0.0810	0.0633	0.1485	0.1094
		RMS	1.3875	1.5165	1.5179	1.4025	1.6375	1.4884
		Time(s)	4.6603	4.6307	4.707	4.5152	4.4056	4.2336
	PICP	$\varepsilon_{\mathbf{R}}$	1.1376e−15	2.4381e−15	9.9997e−16	6.7074e−16	4.8303e−6	2.5428e−5
		ε_t	3.8439e−14	4.4394e−14	3.4914e−14	1.6755e−14	1.9460e−4	5.8369e−4
		RMS	1.1111e−13	2.4014e−13	1.6833e−13	1.1113e−13	0.0627	0.0573
		Time(s)	0.1334	0.1316	0.1301	0.1251	0.1221	0.1277
Bone	ICP	$\varepsilon_{\mathbf{R}}$	0.0120	0.0112	0.0118	0.0092	0.0078	0.0064
		ε_t	2.4571	0.1576	0.1109	0.2109	0.1621	0.0540
		RMS	2.0667	2.0838	2.1146	2.0884	2.0689	2.1266
		Time(s)	0.1606	0.1715	0.1659	0.1651	0.1737	0.1657
	EM–ICP	$\varepsilon_{\mathbf{R}}$	0.0083	0.0072	0.0071	0.0066	0.0054	0.0039
		ε_t	1.7131	0.0964	0.0641	0.1780	0.1243	0.0383
		RMS	1.4041	1.3023	1.3864	1.3944	1.3931	1.3491
		Time(s)	2.7544	2.7323	2.6914	2.6722	2.6942	2.7412
	PICP	$\varepsilon_{\mathbf{R}}$	1.4761e−15	1.1171e−15	1.5374e−15	5.0083e−4	0.0027	7.8080e−6
		ε_t	3.4516e−13	1.0517e−14	1.5657e−14	0.1596	0.0691	0.0203
		RMS	2.0069e−13	1.8633e−13	2.3106e−13	0.4867	1.1232	0.0127
		Time(s)	0.1630	0.1746	0.1755	0.1663	0.1867	01706

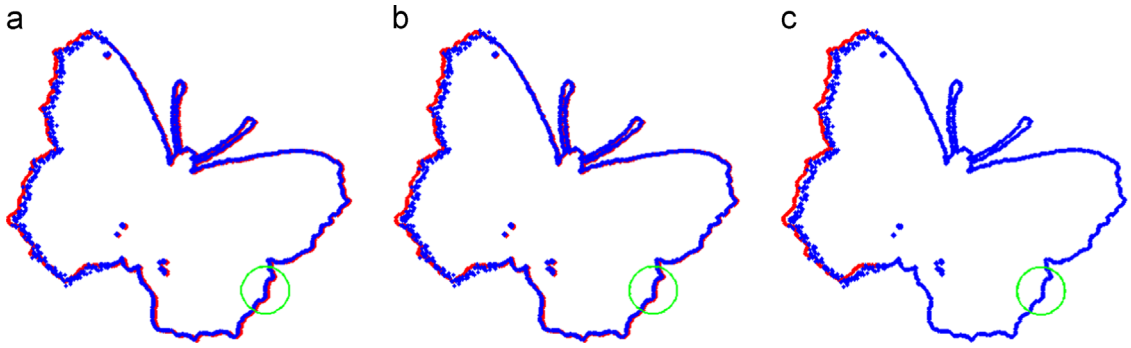

Fig. 3. Registration results of Butterfly. (a) ICP registration result. (b) EM–ICP registration result. (c) PCIP registration result. (For interpretation of the references to color in this figure, the reader is referred to the web version of this article.)

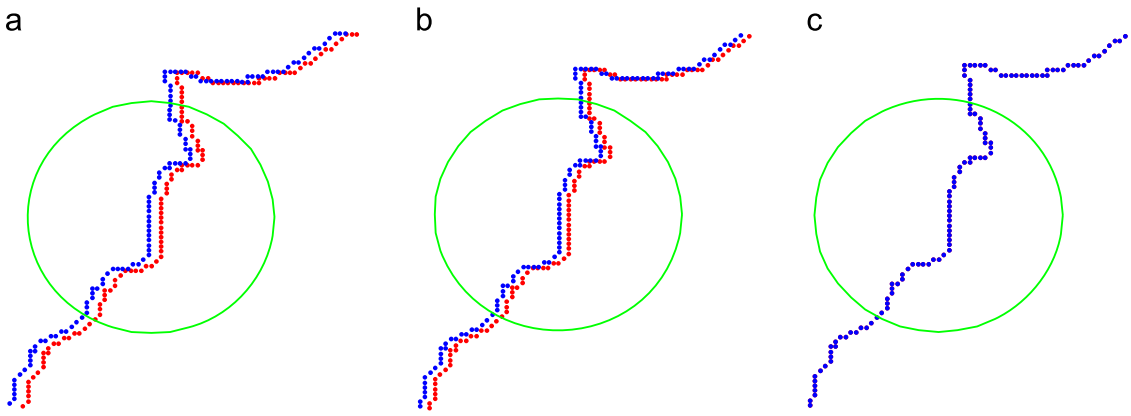

Fig. 4. Local amplification results of Butterfly. (a) Local amplification result of ICP. (b) Local amplification result of EM–ICP. (c) Local amplification result of PICP.

results are reported by RMS. The convergence of three algorithms is analyzed to demonstrate the precision of the proposed algorithm. In addition, the computational efficiency of the three algorithms is presented. The experiments are conducted by Matlab on Intel (R) Core (TM) i7-4770 3.40 GHz CPU, 16.0 GB RAM.

5.1. 2D simulations

In the experiments, 2D images will be rotated and translated by some given values. Rigid transformation got by different registration algorithms is compared with the known rotation matrix and translation vector, and the error is calculated.

Assume the model point set is Y. Given the true rotation matrix R_{true} and the translation vector t_{true}, we can obtain the transformed point set. To prove that our method can deal with noise effectively, we add some shape noise to the transformed point set to get the shape point set X, where the noise abides by the Gaussian distribution.

In the experiments, the 2D Heart, Butterfly and Bone data are used to carry out the experiments. We rotate the data with the angle 10°, 20°, 30°, 40°, 50° and 60° respectively and translate with a random vector in the interval (0, 20). Then the shape noise which has a random mean in the interval (0, 10) and a random variance in the interval (0, 5) is added to 25% of the shape point set. At last, the simulation images are obtained and shown in Fig. 2.

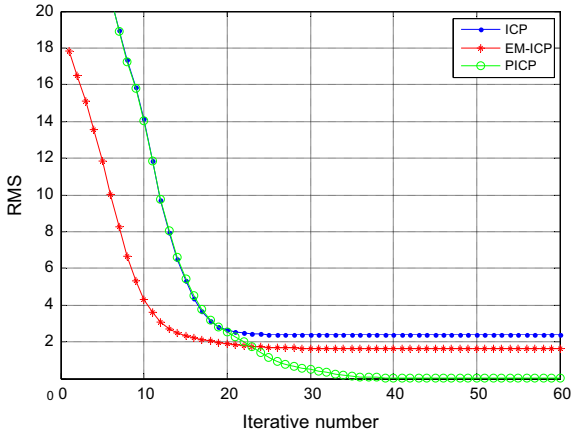

Fig. 5. Registration convergence of ICP, EM–ICP and PICP on Butterfly with noise.

Table 3
RMS and computation time comparison of 2D point sets.

Point sets	ICP		EM–ICP		PICP	
	RMS	Time(s)	RMS	Time(s)	RMS	Time(s)
Heart	9.4081	0.0596	8.8740	2.4381	5.8611e−4	0.1068
Butterfly	0.5148	0.0741	0.4764	3.3729	0.0944	0.1138
Bone	12.6403	0.0416	9.2898	1.8059	0.4161	0.1380

Assuming that we handle the point set with rotation $\mathbf{R}_0$ and translation t_0, according to the regular of matrix and vector, matrix $\mathbf{R}_{true}=\mathbf{R}_0^T$ and vector $t_{true}=-\mathbf{R}_0^T t_0$ can be got. Therefore the relative error of the rotation matrix is $\varepsilon_{\mathbf{R}}=||\mathbf{R}-\mathbf{R}_{true}||_2/||\mathbf{R}_{true}||_2$ and the error of the translation vector is $\varepsilon_t=||t-t_{true}||_2/||t_{true}||_2$. Compared results are presented in the following Table 2.

It can be seen from Table 2 that the error ε_R, ε_t and RMS of PICP algorithm are all the smallest. Compared with the ICP algorithm, PICP algorithm introduces the probability to distinguish effective points and noisy points, as noisy points get small probabilities which can effectively reduce the influence of noise on the registration result. Meanwhile, PICP algorithm is more accurate than the EM–ICP, because the one-to-one correspondence is adopted which expresses the relationship of true point pairs with a large probability which contributes to the high precision, while the probabilities of true point pairs given by full correspondence of EM–ICP algorithm are relatively small because all other false point pairs are given some probabilities which decrease the accuracy. The PICP algorithm has the highest robustness and accuracy proving that the improved approach is effective. Moreover, the computation time of ICP and PICP is quite similar, while the EM–ICP is very time consuming proving that the one-to-one correspondence can improve the efficiency compared with full correspondence.

To clearly and intuitively prove the superiority and accuracy of PICP algorithm, Fig. 3 displays the registration results of Butterfly with 20° rotation. Red and blue point sets respectively represent the model point set and the shape point set after rigid transformation. From Fig. 3, we find that the registration result of PICP is more accurate. To more clearly see the edge of the registration situation, the region marked by circle in Fig. 3 will be amplified in Fig. 4. We can clearly see that noiseless edge registration is very accurate for PICP, but the corresponding edge for ICP and EM–ICP is no complete overlap, illustrating the advantage of PICP algorithm.

Fig. 5 shows the convergence of three kinds of registration algorithms of Butterfly. It can be seen that all these three algorithms are converged and the PICP algorithm obtains the smallest registration error.

Through the study of 2D point sets from simulation data, the registration results and error convergence can prove PICP algorithm for point sets with noise has significant effect. Hence PICP algorithm has the superiority to solve the problem of registering point sets with shape noise.

5.2. 2D standard database

As ε_R and ε_t can not be obtained in the standard database experiments, we just give the RMS and computation time of these three algorithms. In the experiments, Heart, Butterfly and Bone are used, RMS and computation time of the registration results are shown in Table 3. It can be seen that RMS of PICP is the minimum, because

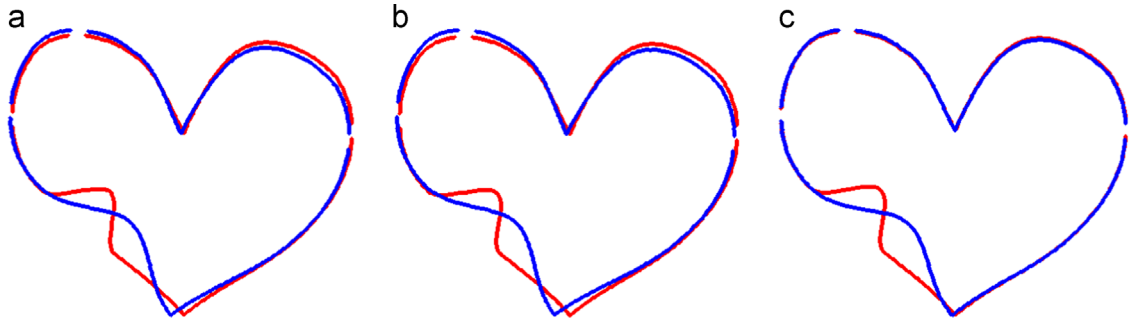

Fig. 6. Registration results of Heart. (a) ICP registration result. (b) EM–ICP registration result. (c) PICP registration result.

when the two shapes are close enough, the weights of noisy points will be smaller and the weights of effective points will be larger greatly reducing the influence of noise on the registration result.

Fig. 6 is the result using different registration algorithms for the data Heart from part B of CE-Shape-1, and it can be seen that PICP registration algorithm performs best and it deals with the noise effectively. Fig. 7 shows the convergence of three kinds of registration algorithms. It can be seen PICP algorithm is more accurate than EM–ICP algorithm, that is because PICP algorithm adopts the one-to-one correspondence which expresses the relationship of true point pairs with a large probability and contributes to the high precision, while the probabilities of true point pairs given by full correspondence of EM–ICP algorithm are relatively small for all other false points occupy some probabilities which decrease the accuracy. In the early stage, the convergence of ICP and PICP is almost the same, because in the beginning Gaussian probability model giving large variance is similar to uniform distribution. Noisy points and effective points have roughly equal probabilities, so PICP algorithm degenerates into ICP algorithm. When two shapes are roughly registered, the value got by EM is used to update Gaussian probability model and improves the convergence precision. PICP gives the best registration, and the reason is when the two image point sets are close enough, the automatically varied Gaussian probability decreases the probabilities of the noisy points and increases the probabilities of the effective points. Therefore, the influence of noise on the result of registration is effectively suppressed and the result is more accurate.

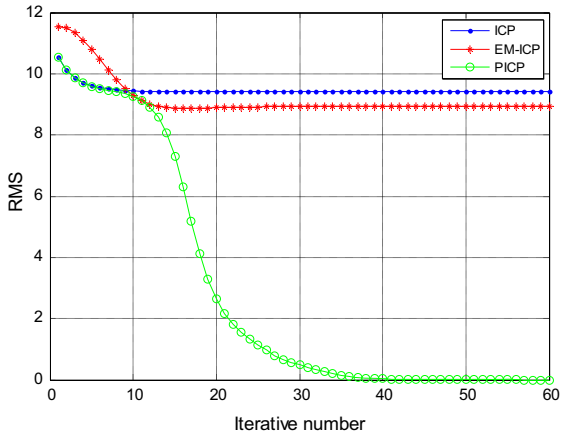

Fig. 7. Registration convergence of ICP, EM–ICP and PICP on Heart with noise.

5.3. 3D simulations

In the 2D experiments, it can be seen the computation time of EM–ICP is far more than ICP and PICP. As the number of 3D data

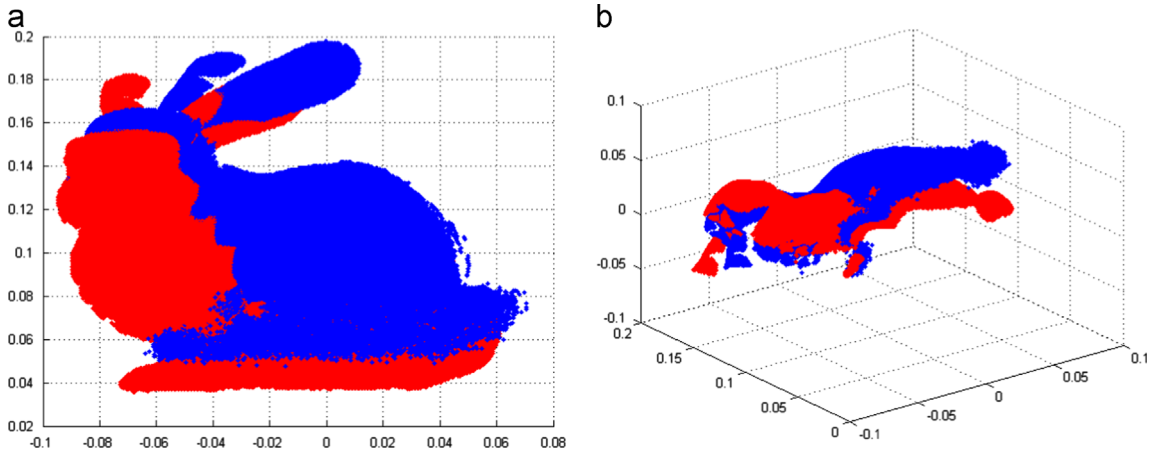

Fig. 8. 2D and 3D view of Bunny for registration. (a) 2D view of Bunny. (b) 3D view of Bunny.

Table 4
Simulation error of 3D point sets.

Point sets	Angle		10	20	30	40	50	60
Dragon	ICP	ε_R	0.0329	0.0313	0.0285	0.0252	0.0213	0.0166
		ε_t	0.3545	0.2683	0.2594	0.2408	0.6215	0.6627
		RMS	0.0030	0.0029	0.0027	0.0026	0.0025	0.0024
	PICP	ε_R	0.0095	0.0117	0.0096	0.0119	0.0076	0.0078
		ε_t	0.0838	0.0642	0.0765	0.0853	0.1632	0.1911
		RMS	1.9322e−6	1.1428e−6	8.3011e−6	3.3914e−7	1.8296e−6	1.5669e−6
Bunny	ICP	ε_R	0.0255	0.0239	0.0234	0.0196	0.0175	0.0139
		ε_t	0.3880	0.4490	0.1930	0.2122	0.2653	0.1546
		RMS	0.0026	0.0025	0.0023	0.0022	0.0022	0.0022
	PICP	ε_R	0.0060	0.0100	0.0097	0.0100	0.0145	0.0100
		ε_t	0.0789	0.1164	0.0477	0.0755	0.1589	0.0683
		RMS	7.8800e−6	7.8283e−6	8.5350e−6	7.4825e−6	6.4777e−6	8.3923e−6
Happy buddha	ICP	ε_R	0.0258	0.0261	0.0247	0.0224	0.0199	0.0157
		ε_t	0.1925	0.2395	0.3192	0.6226	0.2077	0.3518
		RMS	0.0029	0.0027	0.0025	0.0023	0.0022	0.0021
	PICP	ε_R	0.0024	0.0026	0.0099	0.0110	0.0099	0.0124
		ε_t	0.0333	0.0241	0.0238	0.0291	0.0194	0.0678
		RMS	8.4167e−6	7.9843e−6	8.3514e−6	8.3057e−6	8.2662e−6	4.2109e−5

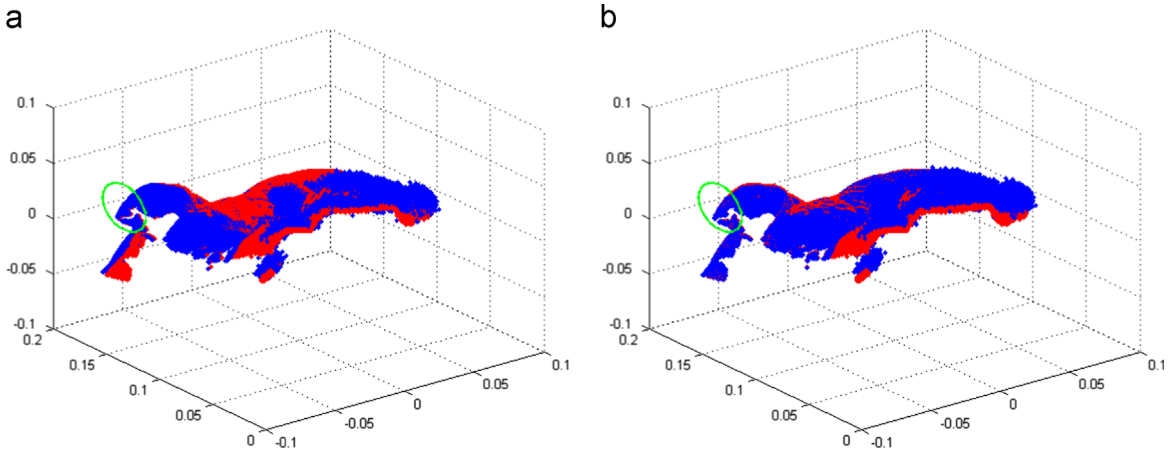

Fig. 9. Registration results of Bunny. (a) ICP registration result. (b) PICP registration result.

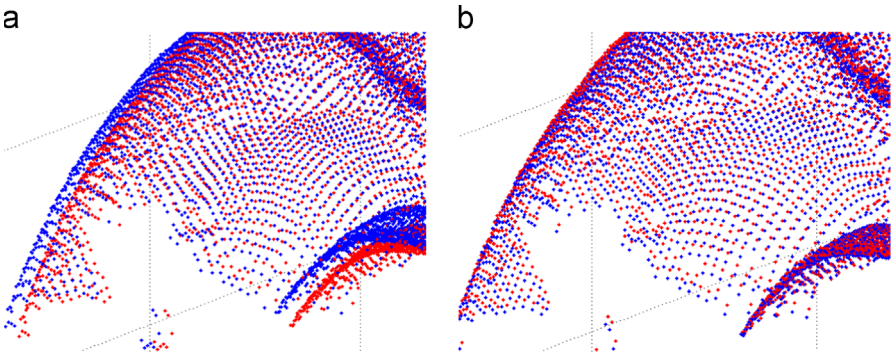

Fig. 10. Local amplification results of Bunny. (a) Local amplification result of ICP. (b) Local amplification result of PICP.

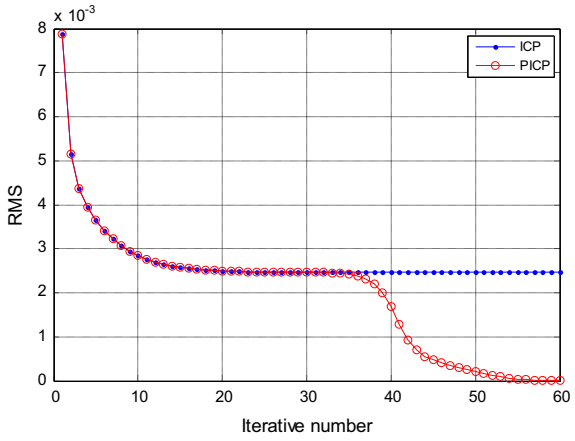

Fig. 11. Registration convergence of ICP and PICP on Bunny with noise.

points is quite large, so EM–ICP is time consuming, we only compare the PICP algorithm with the ICP algorithm. A 3D point set from the Stanford 3D Scanning Repository is chosen as a model point set, and then the model point set is rotated, translated and added noise to get the shape point set. The rigid transformation calculated by the PICP and ICP algorithms is used to compare with the known parameters to estimate accuracy and effectiveness of the algorithms.

The 3D simulation experiment is conducted similar to the 2D simulation experiments. Here we respectively rotate Dragon, Bunny and Happy Buddha 10°, 20°, 30°, 40°, 50° and 60°, and add Gaussian shape noise with a random expectation in the interval (0, 0.020) and a random variance in the interval (0, 0.010) to 25% of the shape point set. Fig. 8 shows 2D and 3D views of Bunny with noise for registration. Table 4 shows the relative error of Dragon, Bunny and Happy Buddha.

In order to more clearly see the results of simulation experiments, the registration results of ICP and PICP of Bunny with 20° rotation are displayed in Fig. 9. It can be verified that PICP registration result is better than ICP. To more clearly see the edge of the registration situation, the parts marked by the green circle are amplified which are showed in Fig. 10.

In Fig. 11 we further observe the registration results of ICP and PICP by error convergence. It can be seen that PICP and ICP have the same weight in the first stage of registration, but when two point sets are close enough, PICP algorithm gives different weights for different pairs according to the distance between point and point. For effective points, distances are short, so they get heavy weight. For noise points, distances are long, so they get small weight. It effectively reduces the impact of noise on registration results making the final registration result accurate (Fig. 12).

5.4. 3D standard database

In this part, 3D range images from the Stanford 3D Scanning Repository are registered, red and blue point sets respectively representing model point set and shape point set.

RMS of Dragon, Bunny and Happy Buddha for ICP and PICP registration algorithms is showed in Table 5. The RMS of PICP is smaller, just like the above 2D data. To more clearly and intuitively

observe the registration result of PICP algorithm, registration results of Dragon are showed in Fig. 13. To compare the registration results intuitively, the local images marked by circle in Fig. 13 are amplified which are shown in Fig. 14. It can be seen edge matched by PICP algorithm is more accurate than ICP, showing that the PICP algorithm for registering 3D point set with noise is effective. Fig. 15 shows error convergence figure. The updating of variance of Gaussian model adopts the idea of from coarse to fine and the one-to-one correspondence is employed, so the algorithm has high accuracy.

Table 5
RMS comparison Of 3D point sets.

	Dragon	Bunny	Happy buddha
ICP	0.0021	0.0020	0.0023
PICP	2.0880e−4	7.1503e−5	6.3736e−5

6. Conclusion

This paper proposes the PICP algorithm based on EM principle to deal with the problem of registering point sets with shape noise. To solve this problem, a Gaussian model is introduced into the rigid registration algorithm, which updates real-time in each

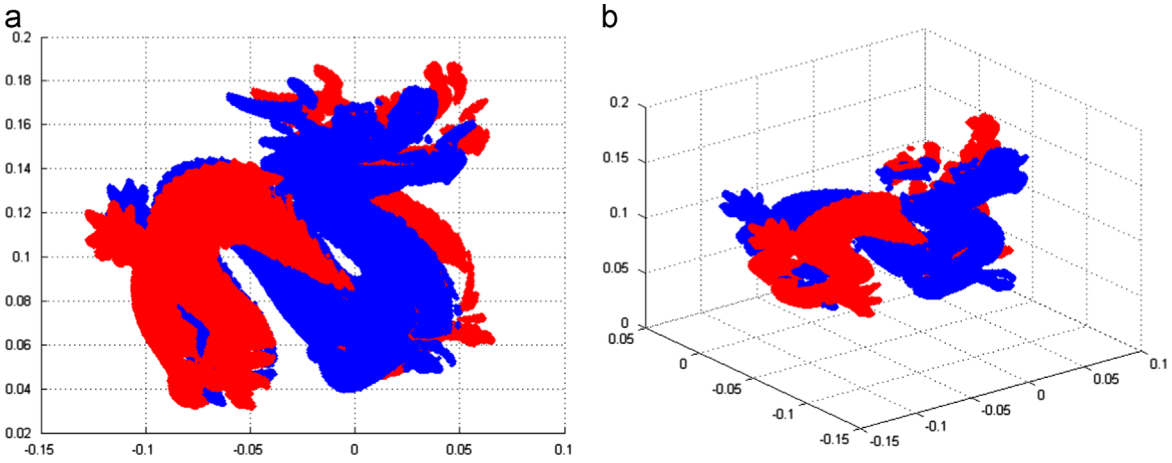

Fig. 12. 2D and 3D view of Dragon for registration. (a) 2D view of Dragon. (b) 3D view of Dragon.

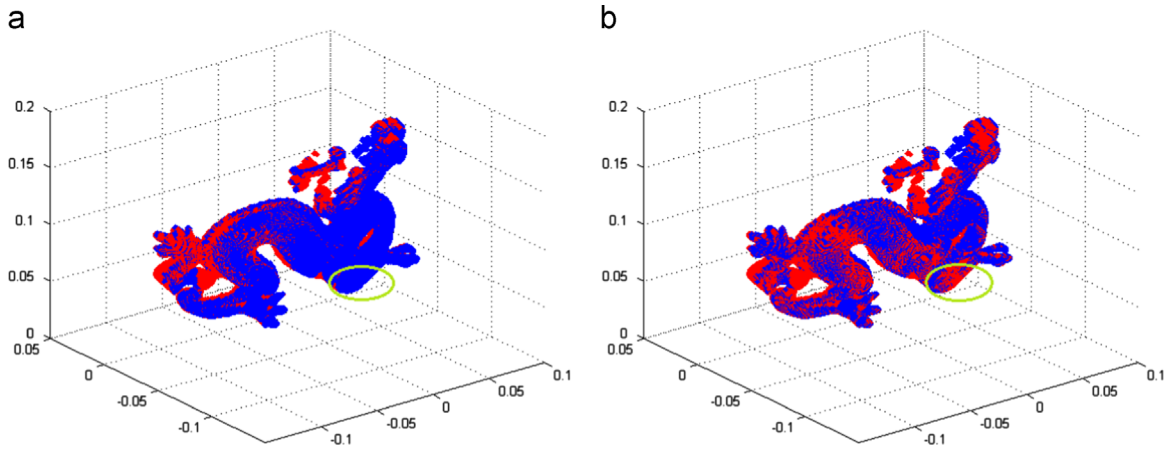

Fig. 13. Registration results of Dragon. (a) ICP registration result. (b) PICP registration result.

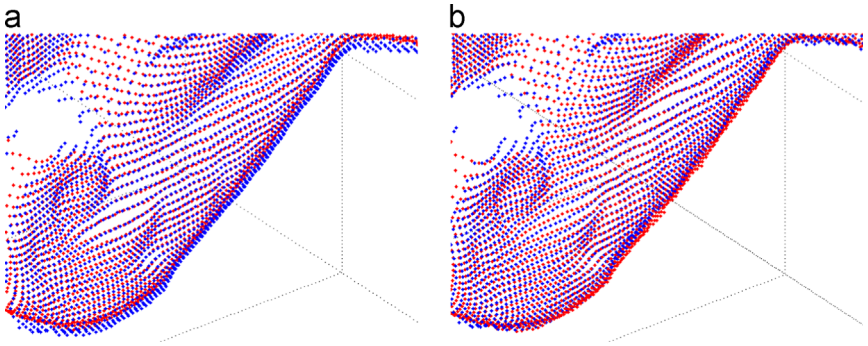

Fig. 14. Local amplification results of Dragon. (a) ICP local amplification result. (b) PICP local amplification result.

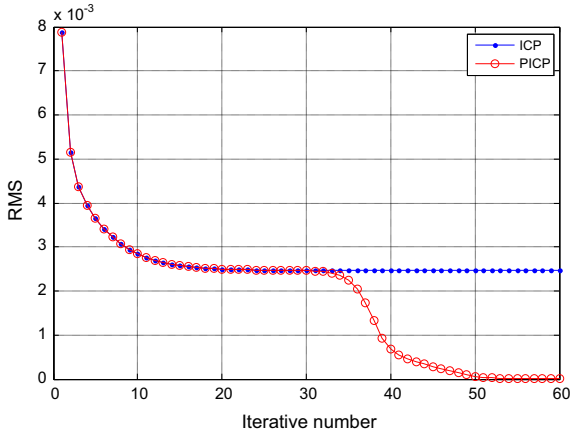

Fig. 15. Registration convergence of ICP and PICP on Dragon with noise.

iteration. Compared with previous works, our algorithm has advantages as following: (1) The one-to-one correspondence is employed to improve the speed, which suppresses the unimportant points and retains the original information of point pairs without the interference of noise. (2) To avoid the proposed algorithm being trapped into the local minimum, the variance of Gaussian probability model is updated from large to small step by step, which can make the registration from coarse to fine. Therefore, the proposed method is much robust and it can achieve much fast speed and high precision. Some experiments of 2D and 3D registration results demonstrate that the PICP performance is better than the ICP and EM–ICP algorithms.

Although the proposed PICP improves the accuracy and speed of *m*-D rigid registration, there are still a lot of other problems needed to be solved such as selecting the annealing coefficient which controls the variance of Gaussian probability model automatically. In the future, the PICP algorithm will be applied to more fields such as the map matching and precise 3D reconstruction.

Acknowledgments

This work was supported by the Natural Science Basic Research Plan in Shaanxi Province of China under Grant no. 2014JM8336, 973 Program under Grant no. 2015CB351703, "the Fundamental Research Funds for the Central Universities" under Grant no. 2013jdhz02, and the National Natural Science Foundation of China under Grant nos. 91320301 and 61231018.

References

[1] Y. Gao, R. Ji, W. Liu, Q. Dai, G. Hua, Weakly supervised visual dictionary learning by harnessing image attributes, IEEE Trans. Image Process. 23 (2014) 5400–5411.
[2] Y. Gao, M. Wang, Z. Zha, J. Shen, X. Li, X. Wu, Visual-textual joint relevance learning for tag-based social image search, IEEE Trans. Image Process. 22 (2013) 363–376.
[3] P.J. Besl, N.D. Mckay, A method for registration of 3-D shapes, IEEE Trans. Pattern Anal. Mach. Intell. 14 (1992) 239–256.
[4] Z. Zhang, Iterative point matching for registration of free-form curves and surfaces, Int. J. Comput. Vis. 13 (1994) 119–152.
[5] Y. Chen, G. Medioni, Object modelling by registration of multiple range images, Image Vis. Comput. 10 (1992) 145–155.
[6] S. Ying, J. Peng, S. Du, H. Qiao, A scale stretch method based on ICP for 3D data registration, IEEE Trans. Autom. Sci. Eng. 6 (2009) 559–565.
[7] S. Du, N. Zheng, S. Ying, J. Liu, Affine iterative closest point algorithm for point set registration, Pattern Recognit. Lett. 31 (2010) 791–799.
[8] B. Combès, S. Prima, Prior affinity measures on matches for ICP-like nonlinear registration of free-form surfaces, in: Proceedings of the IEEE International Symposium on Biomedical Imaging: From Nano to Macro (ISBI), 2009, pp. 370–373.
[9] J. Park, S. Im, K. Lee, J. Lee, Vision-based SLAM system for small UAVs in GPS-denied environments, J. Aerosp. Eng. 25 (2011) 519–529.
[10] D. Kim, D. Kim, A fast ICP algorithm for 3-D human body motion tracking, IEEE Signal Process. Lett. 17 (2010) 402–405.
[11] S. Rusinkiewicz, M. Levoy, Efficient variants of the ICP algorithm, in: Proceedings of the 2001 Third IEEE International Conference on 3-D Digital Imaging and Modeling, 2001, pp. 145–152.
[12] A.W. Fitzgibbon, Robust registration of 2D and 3D point sets, Image Vis. Comput. 21 (2003) 1145–1153.
[13] T. Jost, H. Hugli, A multi-resolution ICP with heuristic closest point search for fast and robust 3D registration of range images, in: Proceedings of the Fourth IEEE International Conference on 3-D Digital Imaging and Modeling (3DIM), 2003, pp. 427–433.
[14] A. Almhdie, C. Léger, M. Deriche, L. Nguyen, R. Lédée, The comprehensive ICP (CICP) algorithm and its application to the multidmoal registration of 3D surfaces of the heart, in: Proceedings of the 15th IEEE International Conference on Systems, Signals and Image Processing (IWSSIP), 2008, pp. 499–502.
[15] C. Zhang, S. Du, J. Xue, X. Qi, Improved ICP algorithm with bounded rotation angle for 2D point set registration, in: Proceedings of the Foundations and Practical Applications of Cognitive Systems and Information Processing, 2014, pp. 523–530.
[16] G.C. Sharp, S.W. Lee, D.K. Wehe, ICP registration using invariant features, IEEE Trans. Pattern Anal. Mach. Intell. 24 (2002) 90–102.
[17] B. Lee, C. Kim, R. Park, An orientation reliability matrix for the iterative closest point algorithm, IEEE Trans. Pattern Anal. Mach. Intell. 22 (2000) 1205–1208.
[18] L. Zhang, S. Choi, S. Park, Robust ICP registration using biunique correspondence, in: Proceedings of the 2011 IEEE International Conference on 3D Imaging, Modeling, Processing, Visualization and Transmission (3DIMPVT), 2011, pp. 80–85.
[19] L. Silva, O.R.P. Bellon, K.L. Boyer, Precision range image registration using a robust surface interpenetration measure and enhanced genetic algorithms, IEEE Trans. Pattern Anal. Mach. Intell. 27 (2005) 762–776.
[20] D. Chetverikov, D. Svirko, D. Stepanov, P. Krsek, The trimmed iterative closest point algorithm, in: Proceedings of the 2002 16th IEEE International Conference on Pattern Recognition, 2002, pp. 545–548.
[21] J.M. Phillips, R. Liu, C. Tomasi, Outlier robust ICP for minimizing fractional RMSD, in: Proceedings of the Sixth IEEE International Conference on 3-D Digital Imaging and Modeling (3DIM), 2007, pp. 427–434.
[22] S. Du, J. Zhu, N. Zheng, Y. Liu, C. Li, Robust iterative closest point algorithm for registration of point sets with outliers, Opt. Eng. 50 (2011) 87001.
[23] D. Rodriguez-Losada, J. Minguez, Improved data association for icp-based scan matching in noisy and dynamic environments, in: Proceedings of the 2007 IEEE International Conference on Robotics and Automation, 2007, pp. 3161–3166.
[24] L. Wei, C. Cappelle, Y. Ruichek, Unscented information filter based multi-sensor data fusion using stereo camera, laser range finder and GPS receiver for vehicle localization, in: Proceedings of the 2011 14th IEEE International Conference on Intelligent Transportation Systems (ITSC), 2011, pp. 1923–1928.
[25] T. Ridene, F. Goulette, Registration of fixed-and-mobile-based terrestrial laser data sets with DSM, in: Proceedings of the IEEE International Symposium on Computational Intelligence in Robotics and Automation (CIRA), 2009, pp. 375–380.
[26] B. Jian, B.C. Vemuri, A robust algorithm for point set registration using mixture of Gaussians, in: Proceedings of the Tenth IEEE International Conference on Computer Vision (ICCV), 2005, pp. 1246–1251.
[27] S. Granger, X. Pennec, Multi-scale EM–ICP: a fast and robust approach for surface registration, in: Proceedings of 7th European Conf. Comput. Vis. (ECCV) (2002) 418–432.
[28] A. Myronenko, X. Song, Point set registration: coherent point drift, IEEE Trans. Pattern Anal. Mach. Intell. 32 (2010) 2262–2275.
[29] C.V. Stewart, C. Tsai, B. Roysam, The dual-bootstrap iterative closest point algorithm with application to retinal image registration, IEEE Trans. Med. Imaging 22 (2003) 1379–1394.
[30] L. Liu, X. Hu, Y. Chen, T. Zhang, M. Li, A new close-form solution for initial registration of ICP, Adv. Mater. Res. 143 (2011) 287–292.
[31] C.B. Barber, D.P. Dobkin, H. Huhdanpaa, The quickhull algorithm for convex hulls, ACM Trans. Math. Softw. (TOMS) 22 (1996) 469–483.
[32] H. Chen, T. Lin, An algorithm to build convex hulls for 3-D objects, J. Chin. Inst. Eng. 29 (2006) 945–952.
[33] M. Greenspan, M. Yurick, Approximate K-D tree search for efficient ICP, in: Proceedings of the Fourth International Conference on3-D Digital Imaging and Modeling (3DIM), 2003, pp. 442–448.
[34] A. Nuchter, K. Lingemann, J. Hertzberg, Cached K-D tree search for ICP algorithms, in: Proceedings of the Sixth IEEE International Conference on 3-D Digital Imaging and Modeling (3DIM), 2007, pp. 419–426.
[35] L. Liu, Y. Chen, T. Zhang, Y. Wang, M. Li, Design and implementation of maxi-linear deviation search algorithm based on improved ICP, Adv. Mater. Res. 143 (2011) 293–297.
[36] L. Liu, Y. Wang, M. Li, Y. Chen, T. Zhang, Maxi-linear deviation searching algorithm based on improved pyramid filter, J. Comput. 6 (2011) 2164–2172.
[37] L.J. Latecki, R. Lakamper, T. Eckhardt, Shape descriptors for non-rigid shapes with a single closed contour, in: Proceedings of the IEEE Conference on Computer Vision and Pattern Recognition, 2000, pp. 424–429.
[38] The Stanford 3D Scanning Repository: ⟨http://graphics.stanford.edu/data/3Dscanrep/⟩.

Shaoyi Du received his Ph.D. degree in pattern recognition and intelligence system from Xi'an Jiaotong University, China in 2009. He is an Associate Professor of Xi'an Jiaotong University. His research interests include computer vision and pattern recognition.

Juan Liu received Bachelor degree in automation from Xi'an Jiaotong University, China in 2013. She is currently a graduate student in the Institute of Artificial Intelligence and Robotics in Xi'an Jiaotong University. Her research interests include mobile robot and image registration.

Chunjia Zhang received Bachelor degree from Nanjing University of Technology, China in 2008. He is currently a Ph.D. Candidate in the Institute of Artificial Intelligence and Robotics in Xi'an Jiaotong University. His research interests include mobile robot and image registration.

Jihua Zhu received his Ph.D. degree in Control Science and Engineering in 2011, from Xi'an Jiaotong University, China. He is an assistant professor of Xi'an Jiaotong University. His research interests include autonomous robots and computer vision.

Ke Li received the Ph.D. degree in Man-machine and Environment Engineering from Beihang University, Beijing, China, in 2008. Currently, he is an assistant professor in the School of Aeronautic Science and Technology, Beijing University of Aeronautics and Astronautics. His current research interests include intelligent control algorithm, process control and simulation of control method.